Journal of
Materials Chemistry A

This article can be cited before page numbers have been issued, to do this please use: Z. Huang, K. Teramura, H. Asakura, S. Hosokawa and T. Tanaka, *J. Mater. Chem. A*, 2017, DOI: 10.1039/C7TA04918H.

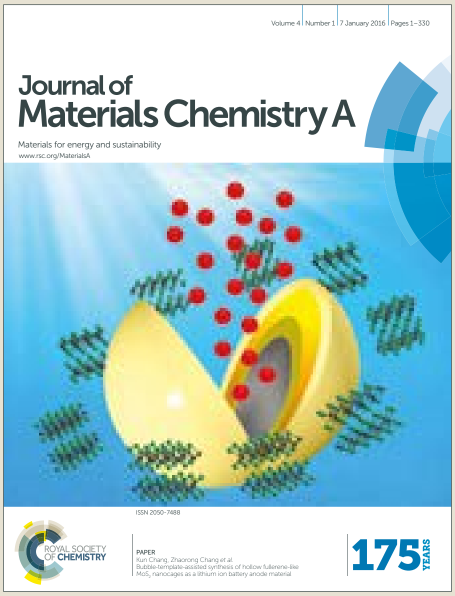

View Article Online
DOI: 10.1039/C7TA04918H

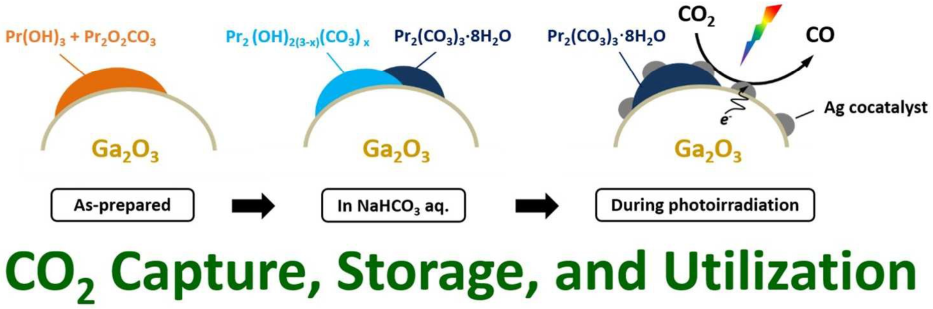

405x146mm (96 x 96 DPI)

View Article Online
DOI: 10.1039/C7TA04918H

Journal Name

ARTICLE

CO_2 capture, storage, and conversion using a praseodymium-modified Ga_2O_3 photocatalyst

Received 00th January 20xx,
Accepted 00th January 20xx

DOI: 10.1039/x0xx00000x

www.rsc.org/

Zeai Huang,[a] Kentaro Teramura,[a,b*] Hiroyuki Asakura,[a,b] Saburo Hosokawa,[a,b] Tsunehiro Tanaka[a,b*]

Praseodymium-modified gallium oxide (Pr/Ga_2O_3) was found to show enhanced activity and selectivity toward CO evolution in the photocatalytic conversion of CO_2 using H_2O as an electron donor in an aqueous solution of $NaHCO_3$ as compared to those of bare Ga_2O_3. The as-prepared Pr species, including $Pr(OH)_3$ and $Pr_2O_2CO_3$, on the surface of Ga_2O_3 were transformed into Pr hydroxycarbonates ($Pr_2(OH)_{2(3-x)}(CO_3)_x$) and Pr carbonate hydrates ($Pr_2(CO_3)_3{\cdot}8H_2O$) in an aqueous solution of $NaHCO_3$, and then the $Pr_2(OH)_{2(3-x)}(CO_3)_x$ was further transformed to $Pr_2(CO_3)_3{\cdot}8H_2O$ with CO_2 bubbling under photoirradiation. This indicates that CO_2 molecules dissolved in water can be captured and stored using Pr species in an aqueous solution of $NaHCO_3$ under CO_2 bubbling. More importantly, $Pr_2(OH)_{2(3-x)}(CO_3)_x$ and $Pr_2(CO_3)_3{\cdot}8H_2O$ accumulated on the surface were decomposed to CO over the Ga_2O_3 photocatalyst with a Ag cocatalyst. Consequently, Ag/Pr/Ga_2O_3 exhibits much higher activity (249 µmol h^{-1} of CO) than the pristine Ag-loaded Ga_2O_3 (136 µmol h^{-1} of CO).

Introduction

CO_2 is a major greenhouse gas and its atmospheric levels have risen quickly during the last decades. This is largely responsible for recent rapid changes in global climate. Carbon capture and storage (CCS) using physical, chemical, and/or biochemical methods is thought to be a safe, effective, and environmentally friendly strategy to mitigate CO_2 emissions.[1-3] However, the development of methods for dealing with the captured CO_2 remains a significant challenge because the desorption and compression of CO_2 after capture is highly energy demanding. Recently, carbon capture and utilization (CCU) has been developed as an alternative approach to CCS.[4-6] Since the captured CO_2 is converted to useful chemicals in the CCU process, CCU has an obvious advantage over CCS. The conversion of CO_2 to chemical feedstocks and hydrocarbon fuels such as carbon monoxide (CO),[7] formic acid (HCOOH),[8] formaldehyde (HCHO),[9] methanol (CH_3OH),[10] and methane (CH_4),[11] have been reported as examples of CCU processes.

Among CO_2 conversion methods, photocatalytic conversion of CO_2 by H_2O as an electron donor with heterogeneous catalysts, which is also known as artificial photosynthesis, is a promising strategy for CCU.[12, 13] Semiconductors activation by light leads to the formation of electrons (e^-) and holes (h^+), which participate in photoreduction and photooxidation, respectively. In such a process, it is important to achieve the stoichiometric oxidation of H_2O, which means that O_2 is evolved equivalently to the reduction products of H_2O and CO_2, thus confirming the role of H_2O as an electron donor. For instance, one mole of H_2O is oxidized by holes to produce four moles of electrons, four moles of protons, and one mole of O_2. Protons and electrons participate in the reduction of CO_2. Thus, the number of holes consumed should be equal to the number of electrons consumed. In addition, the reduction products of CO_2 such as CO, HCOOH, HCHO, CH_3OH, and CH_4 should be the main products instead of H_2. For example, when CO_2 is converted to CO, the selectivity toward CO evolution and the balance between the consumed electrons and holes can be expressed as follows:

$$\text{Selectivity toward CO (\%)} = 100 \times 2\boldsymbol{R}_{\mathbf{CO}} / (2\boldsymbol{R}_{\mathbf{CO}} + 2\boldsymbol{R}_{\mathbf{H2}})$$

$$\text{Consumed } e^-/h^+ = (2\boldsymbol{R}_{\mathbf{CO}} + 2\boldsymbol{R}_{\mathbf{H2}}) / 4\boldsymbol{R}_{\mathbf{O2}}$$

where $\boldsymbol{R}_{\mathbf{CO}}$, $\boldsymbol{R}_{\mathbf{H2}}$, and $\boldsymbol{R}_{\mathbf{O2}}$ represent the rates of CO, H_2, and O_2 formation, respectively. Thus, the selectivity toward CO is preferable when it is higher than 50%, and the consumed e^-/h^+ should be close to 1.0 when H_2O is used as an electron donor. Recently, several catalysts that exhibit activity for the photocatalytic conversion of CO_2 to CO using H_2O as an electron donor have been reported by our group and others.[7, 14-20] Stoichiometric amounts of H_2 and CO were evolved as reduction products, and O_2 was evolved as an oxidation product in all these studies, which means that the number of holes generated and consumed is consistent with that of electrons. Therefore, we have sought to enhance the conversion of CO_2 and selectivity toward CO evolution in the photocatalytic conversion of CO_2 using H_2O as an electron donor.

To achieve high efficiency for the photocatalytic conversion of CO_2, activation of CO_2 by adsorption should be promoted as

---

[a] *Department of Molecular Engineering, Graduate School of Engineering, Kyoto University, Kyotodaigaku Katsura, Nishikyo-ku, Kyoto 615-8510, Japan. E-mail: teramura@moleng.kyoto-u.ac.jp, tanakat@moleng.kyoto-u.ac.jp*

[b] *Elements Strategy Initiative for Catalysts & Batteries (ESICB), Kyoto University, 1-30 Goryo-Ohara, Nishikyo-ku, Kyoto 615-8245, Japan.*

Electronic Supplementary Information (ESI) available. See DOI: 10.1039/x0xx00000x

View Article Online
DOI: 10.1039/C7TA04918H

the first step.[21] Generally speaking, alkali- and alkaline-earth-metal-related materials play important roles in the surface-capture of CO_2 since these materials can be used as solid bases (Lewis basic sites) for the adsorption of CO_2. Alkali- and alkaline-earth-metal-modified photocatalysts have been reported to show enhanced photocatalytic activities for CO_2 conversion using H_2O as an electron donor.[22, 23] CCS on the surface of photocatalysts is desirable for enhancing activity in the photocatalytic conversion of CO_2 as it achieves capture, storage, and conversion of CO_2 in a single step.

Rare-earth (RE) metals can be alternatives to alkali and alkaline earth metals for CO_2 adsorption.[24, 25] Bernal *et al*.[26, 27] reported the behavior of Pr oxides when exposed to air at room temperature. Pr oxides can be transformed into hydroxide and carbonate species on surfaces easily, which indicates that Pr has the potential for CO_2 capture and storage at room temperature. Other kinds of rare-earth elements, such as La,[28] Sm,[29] Nd,[30] Yb,[29] and Y,[31] showed similar abilities to form hydroxide and/or carbonate species on surfaces when exposed to air. More importantly, Borchert *et al*.[32] reported that CO could not be adsorbed on Pr cations, which means that Pr cations could promote CO desorption in the photocatalytic conversion of CO_2 to CO. On the basis of these interesting features, we expected that Pr would be a promising material for the adsorption of CO_2 and desorption of CO. Ga_2O_3 is reported to show good activity for the photocatalytic conversion of CO_2 using H_2O as an electron donor, however, the selectivity toward CO evolution is not satisfied.[7] Thus, the combination of Pr with Ga_2O_3 is expected to be a good strategy for the enhancement of CO evolution. In this work, we present a new strategy for carbon capture, storage, and conversion (CCSC) as a new one-step CCU process in which Pr is used to enhance the CO_2 capture and storage ability of a gallium oxide (Ga_2O_3) surface for subsequent photocatalytic conversion of CO_2 to CO using H_2O as an electron donor.

Experimental

Catalyst preparation

Ga_2O_3 was obtained by the calcination of gallium oxide hydroxides (GaOOH), prepared via the hydrolysis of gallium nitrate ($Ga(NO_3)_3$) with an aqueous solution of ammonia (NH_3), at 1273 K for 6 h. Pr-modified Ga_2O_3 (Pr/Ga_2O_3) was prepared by an impregnation method. Ga_2O_3 was introduced to an aqueous solution of 0.0–10.0 mol% $Pr(NO_3)_3$. The samples were labeled *x* Pr/Ga_2O_3, where *x* denotes the content of Pr as a molar percentage. The suspension was stirred at 353 K for 2 h to evaporate the water. The sample was then calcined at 1223 K for 6 h in air. Praseodymium hydroxide ($Pr(OH)_3$) was fabricated by a typical precipitation method using praseodymium nitrate ($Pr(NO_3)_3$) as a Pr precursor with an aqueous solution of NH_3 at pH 11.0. Praseodymium oxycarbonate ($Pr_2O_2CO_3$) was prepared by calcining the as-prepared $Pr(OH)_3$ at 773 K for 2 h under a CO_2 atmosphere. The fabricated photocatalysts (0.5 g) were modified with 1.0 wt% of a silver (Ag) cocatalyst by a typical photodeposition method, i.e., the photocatalysts were dispersed in an aqueous solution of $AgNO_3$ and then illuminated for 2 h in an Ar flow.

Catalyst characterization

X-ray diffraction (XRD) patterns of the Pr/Ga_2O_3 samples were recorded using a Rigaku Ultima IV powder diffractometer. The UV-Vis diffuse reflectance spectra (UV-vis DRS) were measured with a JASCO V-670 spectrometer equipped with an integrating sphere. Spectralon®, which was supplied by Labsphere Inc., was used as a standard reflection sample. The Pr L_3-edge X-ray absorption fine structure (XAFS) measurements were obtained in transmission and fluorescence modes at the BL01B1 beamline of the SPring-8 synchrotron radiation facility (Hyogo Pref., Japan). Scanning electron microscopy (SEM) images were obtained using a field-emission scanning electron microscope (SU-8220, Hitachi High-Technologies) equipped with an energy-dispersive X-ray spectroscopy (EDS) unit at an acceleration voltage of 15.0 kV. The Brunauer–Emmett–Teller (BET) surface area was measured by N_2 adsorption at 77 K using a volumetric gas adsorption apparatus (BELmini, Bel Japan, Inc.). Temperature programmed desorption of CO_2 (CO_2-TPD) profile was recorded by a TPD-1-AT instrument supplied by the BEL Japan Inc. The samples were heated at a rate of 10 K min^{-1} from 313 K to 1223 K under a He atmosphere.

Photocatalytic activity test for the conversion of CO_2 with H_2O

The photocatalytic conversion of CO_2 using H_2O, including

Table 1 Surface area, CO_2 stored, formation rates of product, selectivity toward CO evolution, and electron balance for the photocatalytic conversion of CO_2 using H_2O as an electron donor.

Entry	Photocatalyst	Surface area / $m^2\ g^{-1}$[a]	CO_2 stored / μmol g^{-1}[b]	Formation rate / μmol h^{-1}[c]			Selec. (%)[d]	e^-/h^+
				H_2	O_2	CO		
1	bare Ga_2O_3	12	7.90	131	124	136	51.0	1.07
2	1.0 Pr/Ga_2O_3	9.4	119	102	148	215	67.7	1.07
3	3.0 Pr/Ga_2O_3	8.9	382	64.7	150.4	249	79.4	1.04
4	5.0 Pr/Ga_2O_3	6.9	425	50.1	128.5	236	82.5	1.11
5	10.0 Pr/Ga_2O_3	8.0	498	39.0	88.9	163	80.7	1.14

[a]BET surface area. [b]Measured by CO_2-TPD. [c]Formation rate after 1 h of irradiation. [d]Selectivity toward CO evolution.

View Article Online
DOI: 10.1039/C7TA04918H

the Ag cocatalyst modification of the photocatalysts, was carried out in a quartz inner-irradiation type reaction vessel (1.0 L) in a quasi-flow batch system. The synthesized photocatalyst (0.5 g) was dispersed in an aqueous solution of $NaHCO_3$ (0.1 M). CO_2 gas (99.999%) was bubbled into the solution at a flow rate of 30 mL min^{-1}. The suspension was irradiated with a 400 W high-pressure mercury lamp through a quartz filter equipped with a cooling water system. The CO, H_2, and O_2 products were analyzed by gas chromatography with thermal conductivity detection (GC-TCD) on a Shimadzu GC-8A chromatograph equipped with a 5Å molecular sieve column (carrier gas: Ar) and by GC with flame ionization detection (FID) with a methanizer and a Shincarbon ST column (carrier gas: N_2).

Results and discussion

Table 1 shows the rate of product formation for the photocatalytic conversion of CO_2 in an aqueous solution of 0.1 M $NaHCO_3$ over Ag/Ga_2O_3 with or without Pr modification. In all cases, CO and H_2 are evolved as the reduction products of CO_2 and H_2O, respectively. Other reduction products, such as CH_4, HCOOH, HCHO, and CH_3OH, were not detected by GC and HPLC in the present study. In addition, almost stoichiometric amounts of O_2 are observed (electron balance was closed to 1.0), indicating the use of H_2O as an electron donor. It should be noted that all the Pr/Ga_2O_3 catalysts show higher CO formation rates than that of bare Ga_2O_3 (0.0 Pr/Ga_2O_3). Therefore, we succeeded in enhancing the photocatalytic activity toward CO evolution using Pr modification. Moreover, the selectivity toward CO evolution is significantly enhanced with different amounts of Pr modification. Notably, 3.0 Pr/Ga_2O_3 shows the highest photocatalytic activity toward CO evolution (249 μmol h^{-1}) in Table 1, which is 1.8 times that over bare Ga_2O_3 (136 μmol h^{-1}). The selectivity toward CO evolution was achieved at 79.4% using 3.0 Pr/Ga_2O_3, which is much higher than using bare Ga_2O_3.

We should note that the surface area is not dependent on the photocatalytic activity toward CO evolution, since the surface areas of all the catalysts were decreased after the Pr modification (Table 1). UV-Vis DR spectra of Pr/Ga_2O_3 showed a slight red shift of absorption edge as compared to that of the bare Ga_2O_3 (Fig. S1); however, it is hard to say that the change of absorption edge affects the photocatalytic activity since the red shift of absorption edge disappeared after reaction (Fig. S2). On the other hand, we estimated amount of CO_2 captured and stored after reaction using the peak area in the CO_2-TPD profile as shown in Table 1. Note that the amount of CO_2 captured and stored over bare Ga_2O_3 was very small (7.9 μmol g^{-1}); however, the Pr modification made it dramatically enhanced. It is discussed that CO_2 dissolved in water is easily captured and stored by the Pr modification. The amount of CO_2 captured and stored did not depend on the photocatalytic formation rate of CO. This phenomenon will be discussed later. The Pr modification effectively enhances the conversion of CO_2 and selectivity toward CO evolution in the photocatalytic conversion of CO_2 by H_2O as an electron donor.

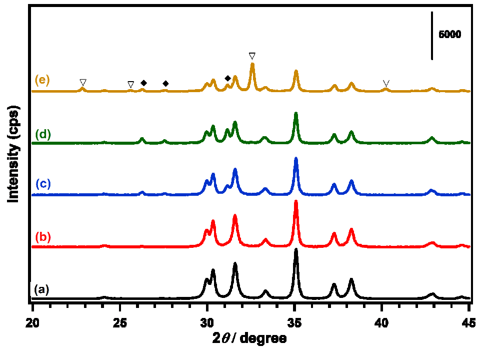

Fig. 1 XRD patterns of Ga_2O_3 with different amounts of Pr: (a) 0 mol%; (b) 1.0 mol%; (c) 3.0 mol%; (d) 5.0 mol%; and (e) 10.0 mol%. Closed diamond: Pr-derived species. Open triangle: $PrGaO_3$.

The XRD patterns of Ga_2O_3 with Pr loadings from 0.0 to 10.0 mol% are shown in Fig. 1. The pattern of bare Ga_2O_3 (0.0 Pr/Ga_2O_3) corresponds to pure β-Ga_2O_3 phase (Fig. 1(a)). No shifts in the diffraction peaks for different amounts of Pr are observed relative to those of Ga_2O_3, therefore, the Pr ions do not act as a dopant in the bulk Ga_2O_3. Several peaks are observed in addition to those assigned to the β-Ga_2O_3 phase when different amounts of Pr are loaded onto Ga_2O_3 (Fig. 1(b–e)). Although the sample was calcined at high temperature in air, these peaks are not consistent with those derived from Pr oxides such as Pr_2O_3 and Pr_6O_{11} (Fig. S3(a) and (b)). Instead, the peaks at 26.3° and 27.5° are very closed to peaks assigned to $Pr_2O_2CO_3$ and $Pr(OH)_3$, respectively (Fig. S3(c) and (d)). As mentioned in the introduction section, Pr hydroxide and carbonate species form readily when Pr oxide is exposed to air.[26, 27] Thus, it is reasonable that these phases of $Pr(OH)_3$ and $Pr_2O_2CO_3$ are formed when a small amount of Pr (0.0–10.0 mol%) is loaded onto Ga_2O_3. Unlike 1.0–5.0 Pr/Ga_2O_3, 10.0 Pr/Ga_2O_3 shows additional peaks that can be easily identified as $PrGaO_3$ (Fig. 1(e)). The peak intensities of the Pr-derived species in 10.0 Pr/Ga_2O_3 are decreased as compared with those of 5.0 Pr/Ga_2O_3. Thus, a high concentration of Pr (10.0 mol%) in the precursor favors the formation of $PrGaO_3$ rather than Pr-derived hydroxide, and carbonate.

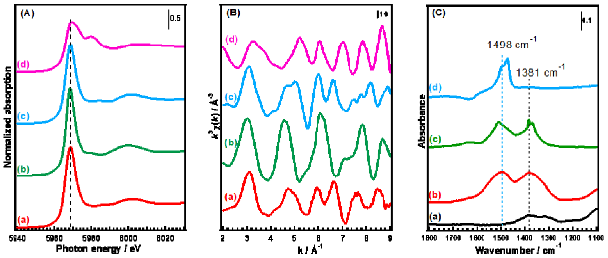

Fig. 2 (A) Pr L_3-edge XANES spectra and (B) EXAFS spectra of (a) 3.0 Pr/Ga_2O_3, (b) $Pr(OH)_3$, (c) $Pr_2O_2CO_3$, and (d) Pr_6O_{11}. (C) FTIR spectra of (a) bare Ga_2O_3, (b) 3.0 Pr/Ga_2O_3, (c) $Pr(OH)_3$, and (d) Pr_2O_2 CO_3.

Fig. 2(A) and 2(B) show the Pr L_3-edge normalized XANES and the k^3-weighted EXAFS spectra of 3.0 Pr/Ga_2O_3, with $Pr(OH)_3$, $Pr_2O(CO_3)_2$, and Pr_6O_{11} as references. The peak

View Article Online
DOI: 10.1039/C7TA04918H

position of the white line in the Pr L_3-edge XANES spectrum of 3.0 Pr/Ga_2O_3 is the same as those of $Pr(OH)_3$, and $Pr_2O(CO_3)_2$ (Fig. 2(a), (b) and (c) in (A)), suggesting that the Pr species in these materials exist in the same average oxidation state, but one that is slightly lower than that of Pr_6O_{11} (Fig. 2(d) in (A)). This is easily understood because the state of Pr in Pr_6O_{11} is actually a mixture of Pr^{3+} and Pr^{4+}, while only Pr^{3+} is contained in our catalysts (Fig. 2(a) in (A)). The k^3-weighted EXAFS spectrum of the 3.0 Pr/Ga_2O_3 is not completely consistent with any of the references; however, parts of the spectrum are similar to those of $Pr(OH)_3$ and $Pr_2O_2CO_3$ at low wavenumber (Fig. 2(B)). In the FTIR spectra of 3.0 Pr/Ga_2O_3 (Fig. 2(C)), the peak at 1381 cm^{-1} corresponding to carbonates was the same as that of $Pr(OH)_3$. As discussed in the introduction section, we expected that $Pr(OH)_3$ was reported to easily adsorb CO_2 in the air and then changed into carbonate.[26, 27, 33] Moreover, the peak at 1498 cm^{-1} is consistent with that of the $Pr_2O_2CO_3$ reference due to the v_3 mode of carbonate. However, in the case of Ga_2O_3, these peaks are rarely observed at this range (Fig. 2(C)). These results indicated that our catalysts contain many kinds of Pr-derived species, $Pr(OH)_3$ and $Pr_2O_2CO_3$ were formed on Ga_2O_3 during the preparation process.

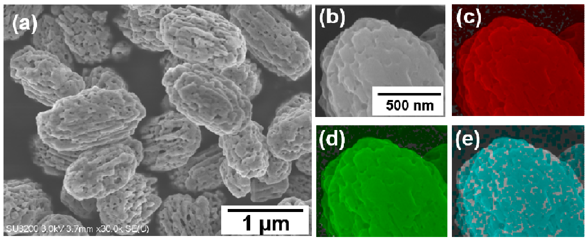

Fig. 3 SEM images of (a) 3.0 Pr/Ga_2O_3, (b) one selected single crystal and corresponding element mapping images for (c) Ga, (d) O, and (e) Pr.

The SEM and related EDS mapping (Fig. 3) of 3.0 Pr/Ga_2O_3 indicate that its elliptical rod-like morphology is maintained as compared to that of Ga_2O_3 (Fig. 3(a) and S4(a)). The amount of Pr shows no obvious effect on the morphology and grain size of the Ga_2O_3 (Figs. 3(a) and S4). The sizes of the Ga_2O_3 particles with different amount of Pr are all around 1 µm. Thus, particle size has no obvious effect on activity in the photocatalytic conversion of CO_2. The Ga and O elements were well mapped with its morphology using a single crystal of 3.0 Pr/Ga_2O_3 (Fig. 3(b)–(d)). The EDS mapping confirms that Pr is well dispersed on the Ga_2O_3 (Fig. 3(e)). Based on the XRD, XAFS, FTIR, and SEM results, $Pr(OH)_3$ and $Pr_2O_2CO_3$ are found to be well loaded on the surface of the Ga_2O_3 as a natural CO_2 capture and storage material, which should enhance its activity for the photocatalytic conversion of CO_2 by H_2O.

The XRD patterns of Pr/Ga_2O_3 with different amounts of Pr after 5 h of photoirradiation are shown in Fig. 4. There is no difference before and after the photocatalytic conversion of CO_2 over bare Ga_2O_3 (0.0 Pr/Ga_2O_3) (Figs. 1(a) and 4(a)). This is not surprising as β-Ga_2O_3 is very stable under photoirradiation. Interestingly, all the peaks assigned to the as-prepared Pr-derived species such as $Pr(OH)_3$ and $Pr_2O_2CO_3$ in 1.0 and 3.0 Pr/Ga_2O_3 completely disappear after 5 h of photoirradiation. In addition, some new peaks derived from $Pr_2(CO_3)_3{\cdot}8H_2O$ appear in the XRD patterns of Pr/Ga_2O_3.[34] This means that $Pr(OH)_3$ and $Pr_2O_2CO_3$ react with other species in the solution to form $Pr_2(CO_3)_3{\cdot}8H_2O$ during the reaction. In the case of 5.0 Pr/Ga_2O_3, the peak at 31.2° assigned to the as-prepared Pr-derived species remains after 5 h of photoirradiation (Figs. 1(d) and 4(d)), and the intensities of the peaks assigned to $Pr_2(CO_3)_3{\cdot}8H_2O$ are much lower than that of 3.0 Pr/Ga_2O_3, indicating that a high concentration of Pr on the Ga_2O_3 hinders the conversion of $Pr(OH)_3$ and $Pr_2O_2CO_3$ to $Pr_2(CO_3)_3{\cdot}8H_2O$ during the reaction. It was also found that $PrGaO_3$ species do not readily change since all the peaks for $PrGaO_3$ are still present for 10.0 Pr/Ga_2O_3 and the related intensities of these peaks are not significantly decreased (Figs. 1(e) and 4(e)). These results show that $Pr(OH)_3$ and $Pr_2O_2CO_3$ on Ga_2O_3 at low concentration (1.0 and 3.0 mol%) tend to completely change to $Pr_2(CO_3)_3{\cdot}8H_2O$ (Fig. 4(b) and (c)), while those at high concentration of Pr (5.0 and 10.0 mol%) do not completely change to $Pr_2(CO_3)_3{\cdot}8H_2O$ after 5 h of photoirradiation (Fig. 4(d) and (e)). Thus, it is important to use a suitably low amount of Pr on the surface of the Ga_2O_3 to enable efficient CO_2 capture and storage.

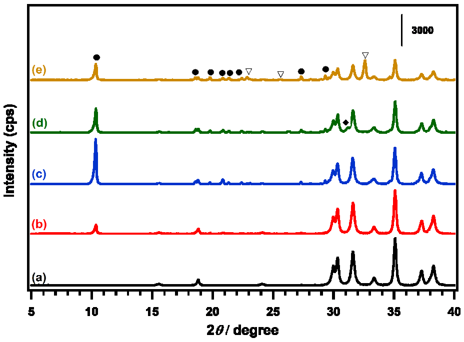

Fig. 4 XRD patterns of Ga_2O_3 with different amounts of Pr after photocatalytic conversion of CO_2: (a) 0 mol%; (b) 1.0 mol%; (c) 3.0 mol%; (d) 5.0 mol%; and (e) 10.0 mol%. Closed circle: $Pr_2(CO_3)_3{\cdot}8H_2O$. Open triangle: $PrGaO_3$. Closed diamond: Pr-derived species.

To ascertain why $Pr(OH)_3$ and $Pr_2O_2CO_3$ are changed to $Pr_2(CO_3)_3{\cdot}8H_2O$ after the reaction, the as-prepared 3.0 Pr/Ga_2O_3 was treated under various conditions. Considering that $NaHCO_3$ and CO_2 are two crucial factors in the formation of rare-earth carbonates,[25, 26, 28] the treatment conditions for samples in aqueous solutions were changed step by step. Fig. 5 denotes the XRD pattern of 3.0 Pr/Ga_2O_3 treated under various conditions. When 3.0 Pr/Ga_2O_3 treated in water under flowing Ar for 5 h, there is no change in the XRD patterns before and after the treatment (Figs. 1(c) and 5(a)), indicating that $Pr(OH)_3$ and $Pr_2O_2CO_3$ are very stable in pure water. In contrast, the peaks assigned to $Pr(OH)_3$ and $Pr_2O_2CO_3$ disappear completely under flowing CO_2 in water (Fig. 5(b)). Since basic $Pr(OH)_3$ species exist in 3.0 Pr/Ga_2O_3 (Figs. 1(c) and 2), and the pH changes from 7.21 under flowing Ar to 3.89 under flowing CO_2 in water, it is not surprising that these species disappear after

View Article Online
DOI: 10.1039/C7TA04918H

reaction owing to the corrosion of these basic species under acidic conditions.

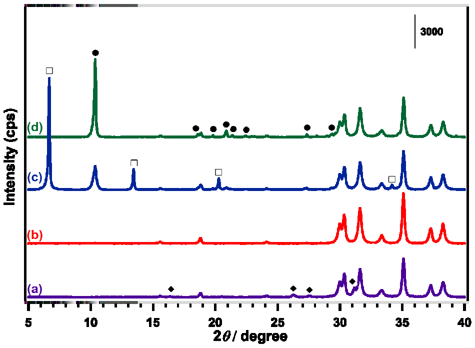

Fig. 5 XRD patterns of 3.0 Pr/Ga_2O_3 dispersed for 5 h in water under (a) Ar flow and (b) CO_2 flow; and in 0.1 M $NaHCO_3$ aqueous solution under (c) Ar flow and (d) CO_2 flow. Closed circle: $Pr_2(CO_3)_3{\cdot}8H_2O$. Closed square: Pr hydroxycarbonates ($Pr_2(OH)_{2(3\text{-}x)}(CO_3)_x$). Closed diamond: Pr-derived species.

Interestingly, all the peaks of $Pr(OH)_3$ and $Pr_2O_2CO_3$ are replaced by new peaks in an aqueous solution of $NaHCO_3$ under a flow of gaseous Ar (Fig. 5(c)). These peaks could be assigned to $Pr_2(OH)_{2(3\text{-}x)}(CO_3)_x$ and $Pr_2(CO_3)_3{\cdot}8H_2O$. It has been reported that rare-earth hydroxycarbonates are easily formed at pH > 6.0 and with a low concentration of CO_2 released from urea.[35] Rare-earth carbonate hydrates are formed in an aqueous solution of $NaHCO_3$ using $Pr(NO_3)_3$ as a precursor.[36] Thus, it is reasonable that both $Pr_2(OH)_{2(3\text{-}x)}(CO_3)_x$ and $Pr_2(CO_3)_3{\cdot}8H_2O$ are formed in the $NaHCO_3$ solution under Ar flow (pH = 8.3). Notably, 3.0 Pr/Ga_2O_3 treated in 0.1 M $NaHCO_3$ under flowing CO_2 show the same phases (a mixture of $Pr_2(CO_3)_3{\cdot}8H_2O$ and Ga_2O_3) as those of 3.0 Pr/Ga_2O_3 after the reaction (Figs. 4(c) and 5(d)), suggesting that the change of $Pr(OH)_3$ and $Pr_2O_2CO_3$ to $Pr_2(CO_3)_3{\cdot}8H_2O$ is due to not photoirradiation but the $NaHCO_3$ solution with flowing CO_2. Pure $Pr(OH)_3$ is also found to change to $Pr_2(CO_3)_3{\cdot}8H_2O$ in 0.1 M $NaHCO_3$ under flowing CO_2 in 20 h (Fig. S5). Thus, there is no doubt that new Pr species such as $Pr_2(OH)_{2(3\text{-}x)}(CO_3)_x$ and $Pr_2(CO_3)_3{\cdot}8H_2O$ are generated on Ga_2O_3 in an aqueous solution of $NaHCO_3$, and then $Pr_2(OH)_{2(3\text{-}x)}(CO_3)_x$ is further transformed to $Pr_2(CO_3)_3{\cdot}8H_2O$ alone under flowing CO_2. We conclude that $Pr(OH)_3$ and $Pr_2O_2CO_3$ can capture and store CO_2 molecules dissolved in an aqueous solution of $NaHCO_3$, and then $Pr_2(OH)_{2(3\text{-}x)}(CO_3)_x$ and $Pr_2(CO_3)_3{\cdot}8H_2O$ are generated on the surface of the Ga_2O_3.

It is important to confirm whether $Pr_2(OH)_{2(3\text{-}x)}(CO_3)_x$ and $Pr_2(CO_3)_3{\cdot}8H_2O$ formed on the surface of Ga_2O_3 can be decomposed by photoirradiation. Thus, 3.0 Pr/Ga_2O_3 was treated in $NaHCO_3$ solution with flowing Ar or CO_2 to obtain $Pr_2(OH)_{2(3\text{-}x)}(CO_3)_x$ and/or $Pr_2(CO_3)_3{\cdot}8H_2O$-modified Ga_2O_3. These catalysts were used for decomposition tests without neither the addition of $NaHCO_3$ nor flowing CO_2, while the other conditions were not changed. Fig. 6 shows the formation rate of CO for the decomposition of $Pr_2(OH)_{2(3\text{-}x)}(CO_3)_x$ and $Pr_2(CO_3)_3{\cdot}8H_2O$ under photoirradiation using 3.0 Pr/Ga_2O_3 with a Ag cocatalyst pretreated using different methods. Bare Ga_2O_3 with and without pretreatment exhibits negligible CO evolution (Fig. 6(a) and (b)). Conversely, the as-prepared 3.0 Pr/Ga_2O_3 is active for the decomposition of Pr-derived species, and CO is observed during photoirradiation (Fig. 6(c)). As discussed above, $Pr_2O_2CO_3$ on Ga_2O_3 is a carbon-containing species. Therefore, it is possible that CO can be formed with a Ag cocatalyst during photoirradiation. Pr/Ga_2O_3 pretreated in $NaHCO_3$ with Ar shows higher CO formation rate than that of as-prepared Pr/Ga_2O_3 (Fig. 6(c) and (d)). Furthermore, the CO evolution rate is highest for Pr/Ga_2O_3 pretreated in $NaHCO_3$ with flowing CO_2 (Fig. 6(e)). We conclude that $Pr_2(OH)_{2(3\text{-}x)}(CO_3)_x$ and $Pr_2(CO_3)_3{\cdot}8H_2O$ can be decomposed to CO during photoirradiation. From this result, it is clearly that only Ga_2O_3 shows no ability for the surface capture and storage of aqueous CO_2 molecules. In contrast, CO_2 capture and storage can be easily performed on Pr/Ga_2O_3, and it can be decomposed to CO during photoirradiation.

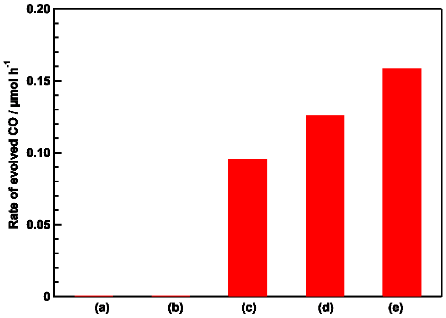

Fig. 6 Formation rate of CO using bare Ga_2O_3 (a) without pretreatment, (b) pretreated in 0.1 M $NaHCO_3$ under flowing CO_2; and using 3.0 Pr/Ga_2O_3 (c) without pretreatment, and pretreated in 0.1 M $NaHCO_3$ under (d) flowing Ar and (e) flowing CO_2. Weight: 0.5 g; Ar flow: 30 mL min^{-1}; solution: 1.0 L pure water; light source: 400 W Hg lamp; Ag loading: 1.0 wt%.

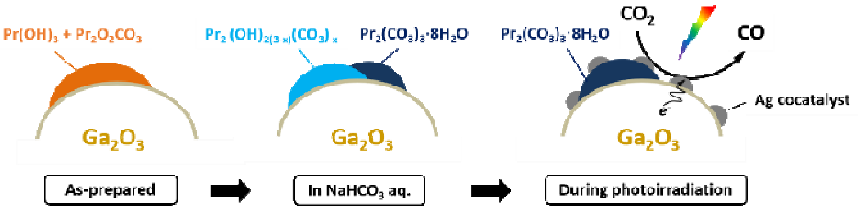

Scheme 1 Formation of Pr-species as a CO_2 capture and storage material in an aqueous solution of $NaHCO_3$.

View Article Online
DOI: 10.1039/C7TA04918H

We proposed a probable mechanism for the capture, storage, and conversion of CO_2 over Ag/Pr/Ga_2O_3 in Scheme 1. $Pr(OH)_3$ and $Pr_2O_2CO_3$ are formed on the surface of Ga_2O_3 after calcination in air when a suitable amount of Pr is loaded onto the Ga_2O_3. $Pr(OH)_3$ and $Pr_2O_2CO_3$ are partially converted into $Pr_2(OH)_{2(3-x)}(CO_3)_x$ and $Pr_2(CO_3)_3{\cdot}8H_2O$ in an aqueous solution of $NaHCO_3$. Accordingly, it is expected that $Pr(OH)_3$ and $Pr_2O_2CO_3$ function as CO_2 capture and storage materials, i.e., $Pr_2(OH)_{2(3-x)}(CO_3)_x$ and/or $Pr_2(CO_3)_3{\cdot}8H_2O$ derived from $Pr(OH)_3$, $Pr_2O_2CO_3$, $NaHCO_3$, and CO_2 on the surface of the Ga_2O_3 are decomposed to CO with a Ag cocatalyst under photoirradiation. Therefore, the photocatalytic activity and selectivity toward CO are dramatically increased, and the H_2 evolution is suppressed, as compared to those of bare Ga_2O_3 due to the CO_2 storage ability of $Pr_2(OH)_{2(3-x)}(CO_3)_x$ and/or $Pr_2(CO_3)_3{\cdot}8H_2O$ on the surface of the Ga_2O_3.

The release and storage of CO_2 were performed stably with three times repetition (Fig. S6). As mentioned in Fig. 3, $Pr_2(CO_3)_3{\cdot}8H_2O$ was formed from $Pr(OH)_3$ and $Pr_2O_2CO_3$ during the reaction. The peaks corresponding to $Pr_2(CO_3)_3{\cdot}8H_2O$ appeared in the XRD pattern of 3.0 Pr/Ga_2O_3 (Fig. S6(a)), and then vanished after the calcination at 1223 K for 1 h (Fig. S6(b)). Interestingly, the peaks reappeared when 3.0 Pr/Ga_2O_3 calcined was retreated in an aqueous solution of $NaHCO_3$ under CO_2 bubbling (Fig. S6(c)). The phenomena were observed approximately reversibly (Fig. S6(d) and (e)). The small peak corresponding to $PrGaO_3$ appeared because the sample was regenerated at high temperature. Amounts of CO_2 captured and stored as $Pr_2(OH)_{2(3-x)}(CO_3)_x$ and $Pr_2(CO_3)_3{\cdot}8H_2O$ were estimated using CO_2-TPD profiles (Fig. S7). All the samples after the reaction (the 1st run), and calcination and treatment in an aqueous solution of $NaHCO_3$ under CO_2 bubbling (the 2nd and 3rd runs) were pretreated under the vacuum at 373 K for 1 h before the CO_2-TPD measurement. The shapes of peaks were not different from each other. On the other hand, the areas of peak slightly decreased with the repetition treatments. The amounts of CO_2 captured and stored in the 1st, 2nd, and 3rd runs were 382, 325, and 269 μmol g^{-1}, respectively. As mentioned above, the capability of Pr/Ga_2O_3 for capture and storage of CO_2 steadily decreased due to the formation of $PrGaO_3$ by the high temperature treatment. We should note that the actual photocatalytic conversion of CO_2 by H_2O was handled at ambient temperature; therefore, CO_2 can be captured, stored, and released to active sites during the photocatalytic reaction without the formation of $PrGaO_3$.

Blank tests were performed to confirm that all these conditions (Fig. S8), including the photocatalyst, photoirradiation, CO_2 flow, Ag co-catalyst, and $NaHCO_3$ additive, are necessary to achieve high photocatalytic activity and selectivity toward CO evolution for CO_2 conversion using H_2O as an electron donor. Therefore, we have succeeded in photocatalytic conversion of CO_2 to CO using Pr/Ga_2O_3, which demonstrates that the CO_2 CCSC process is a viable new alternative to the CCU process.

Conclusions

The modification of Ga_2O_3 with Pr improved the rate of CO formation in the photocatalytic conversion of CO_2 using H_2O as an electron donor. $Pr(OH)_3$ and $Pr_2O_2CO_3$, which are formed on the surface of Ga_2O_3 after the preparation process, function as a CO_2 capture and storage material and produce $Pr_2(OH)_{2(3-x)}(CO_3)_x$ and/or $Pr_2(CO_3)_3{\cdot}8H_2O$ in an aqueous solution of $NaHCO_3$. $Pr_2(OH)_{2(3-x)}(CO_3)_x$ and/or $Pr_2(CO_3)_3{\cdot}8H_2O$ supply CO_2 molecules to the active sites of the Ag cocatalyst and/or Ga_2O_3. Consequently, Ag/Pr/Ga_2O_3 shows a much higher rate of CO formation than Ag-loaded Ga_2O_3. Five blank tests verified that the CO_2 introduced in the gas phase is reduced to CO under photoirradiation. Thus, we succeeded in designing a novel CCU process in which CO_2 is captured, stored on the surface of Ga_2O_3, and converted into a useful chemical feedstock photocatalytically.

Acknowledgements

This study was partially supported by a Grant-in-Aid for Scientific Research on Innovative Areas “All Nippon Artificial Photosynthesis Project for Living Earth” (No. 2406) from the Ministry of Education, Culture, Sports, Science, and Technology (MEXT) of Japan, the Precursory Research for Embryonic Science and Technology (PRESTO), supported by the Japan Science and Technology Agency (JST), and the Program for Elements Strategy Initiative for Catalysts & Batteries (ESICB), commissioned by the MEXT of Japan. The XAFS experiments were performed at a public beamline BL01B1 in SPring-8 with the approval of JASRI (Proposal No. 2015A1764). Zeai Huang thanks the State Scholarship of China Scholarship Council, affiliated with the Ministry of Education of the P. R. China.

Notes and references

1. D. Woolf, J. E. Amonette, F. A. Street-Perrott, J. Lehmann and S. Joseph, *Nature communications*, 2010, **1**, 56.
2. M. D. Jensen, P. Pei, A. C. Snyder, L. V. Heebink, L. S. Botnen, C. D. Gorecki, E. N. Steadman and J. A. Harju, *Energy & Fuels*, 2013, **27**, 4175-4182.
3. A. Goeppert, M. Czaun, R. B. May, G. S. Prakash, G. A. Olah and S. Narayanan, *Journal of the American Chemical Society*, 2011, **133**, 20164-20167.
4. Y.-N. Li, L.-N. He, A.-H. Liu, X.-D. Lang, Z.-Z. Yang, B. Yu and C.-R. Luan, *Green Chemistry*, 2013, **15**, 2825-2829.
5. J. Kothandaraman, A. Goeppert, M. Czaun, G. A. Olah and G. S. Prakash, *Journal of the American Chemical Society*, 2016, **138**, 778-781.
6. A. Otto, T. Grube, S. Schiebahn and D. Stolten, *Energy & environmental science*, 2015, **8**, 3283-3297.
7. K. Teramura, Z. Wang, S. Hosokawa, Y. Sakata and T. Tanaka, *Chemistry-A European Journal*, 2014, **20**, 9906-9909.
8. D. Preti, C. Resta, S. Squarcialupi and G. Fachinetti, *Angewandte Chemie International Edition*, 2011, **50**, 12551-12554.

View Article Online
DOI: 10.1039/C7TA04918H

9. S. Bontemps, L. Vendier and S. Sabo-Etienne, *Journal of the American Chemical Society*, 2014, **136**, 4419-4425.
10. G. Ménard and D. W. Stephan, *Journal of the American Chemical Society*, 2010, **132**, 1796-1797.
11. F. Sastre, A. V. Puga, L. Liu, A. Corma and H. García, *Journal of the American Chemical Society*, 2014, **136**, 6798-6801.
12. S. Sato, T. Arai and T. Morikawa, *Inorganic chemistry*, 2015, **54**, 5105-5113.
13. S. Xie, Q. Zhang, G. Liu and Y. Wang, *Chem Commun*, 2016, **52**, 35-59.
14. Z. Huang, K. Teramura, S. Hosokawa and T. Tanaka, *Appl Catal B-Environ*, 2016, **199**, 272-281.
15. Z. Wang, K. Teramura, S. Hosokawa and T. Tanaka, *Journal of Materials Chemistry A*, 2015, **3**, 11313-11319.
16. S. Iguchi, K. Teramura, S. Hosokawa and T. Tanaka, *Catalysis Today*, 2015, **251**, 140-144.
17. S. Iguchi, K. Teramura, S. Hosokawa and T. Tanaka, *Catalysis Science & Technology*, 2016, **6**, 4978-4985.
18. K. Iizuka, T. Wato, Y. Miseki, K. Saito and A. Kudo, *Journal of the American Chemical Society*, 2011, **133**, 20863-20868.
19. T. Takayama, K. Tanabe, K. Saito, A. Iwase and A. Kudo, *Phys Chem Chem Phys*, 2014, **16**, 24417-24422.
20. H. Yoshida, L. K. Zhang, M. Sato, T. Morikawa, T. Kajino, T. Sekito, S. Matsumoto and H. Hirata, *Catalysis Today*, 2015, **251**, 132-139.
21. X. Chang, T. Wang and J. Gong, *Energy & Environmental Science*, 2016, **9**, 2177-2196.
22. S. Xie, Y. Wang, Q. Zhang, W. Deng and Y. Wang, *ACS Catalysis*, 2014, **4**, 3644-3653.
23. K. Teramura, H. Tatsumi, Z. Wang, S. Hosokawa and T. Tanaka, *Bulletin of the Chemical Society of Japan*, 2015, **88**, 431-437.
24. S. Bernal, G. Blanco, J. Calvino, J. P. Omil and J. Pintado, *Journal of alloys and compounds*, 2006, **408**, 496-502.
25. E. Külah, L. Marot, R. Steiner, A. Romanyuk, T. A. Jung, A. Wäckerlin and E. Meyer, *Scientific Reports*, 2017, **7**, 43369.
26. S. Bernal, F. Botana, R. Garcia and J. Rodriguez-Izquierdo, *Reactivity of solids*, 1987, **4**, 23-40.
27. S. Bernal, F. Botana, G. Cifredo, J. Calvino, A. Jobacho and J. Rodriguez-Izquierdo, *Journal of alloys and compounds*, 1992, **180**, 271-279.
28. P. Fleming, R. A. Farrell, J. D. Holmes and M. A. Morris, *Journal of the American Ceramic Society*, 2010, **93**, 1187-1194.
29. R. Alvero, I. Carrizosa, J. Odriozola, J. Trillo and S. Bernal, *Journal of the Less Common Metals*, 1983, **94**, 139-144.
30. S. Bernal, F. Botana, R. Garcia and J. Rodriguez-Izquierdo, *J Mater Sci*, 1988, **23**, 1474-1480.
31. Y. Kuroda, H. Hamano, T. Mori, Y. Yoshikawa and M. Nagao, *Langmuir*, 2000, **16**, 6937-6947.
32. Y. Borchert, P. Sonström, M. Wilhelm, H. Borchert and M. Bäumer, *The Journal of Physical Chemistry C*, 2008, **112**, 3054-3063.
33. J.-G. Kang, B.-K. Min and Y. Sohn, *Journal of Alloys and Compounds*, 2015, **619**, 165-171.
34. M. Popa and M. Kakihana, *Solid State Ionics*, 2001, **141**, 265-272.
35. L. M. d'Assuncao, I. Giolito and M. Ionashiro, *Thermochimica Acta*, 1989, **137**, 319-330.
36. K. Nagashima, H. Wakita and A. Mochizuki, *Bulletin of the Chemical Society of Japan*, 1973, **46**, 152-156.